AEM
Journals.ASM.org

Light-Dependent Functions of the *Fusarium fujikuroi* CryD DASH Cryptochrome in Development and Secondary Metabolism

Marta Castrillo, Jorge García-Martínez, Javier Avalos

Department of Genetics, Faculty of Biology, University of Seville, Seville, Spain

DASH (*Drosophila*, *Arabidopsis*, *Synechocystis*, human) cryptochromes (cry-DASHs) constitute a subgroup of the photolyase cryptochrome family with diverse light-sensing roles, found in most taxonomical groups. The genome of *Fusarium fujikuroi*, a phytopathogenic fungus with a rich secondary metabolism, contains a gene encoding a putative cry-DASH, named CryD. The expression of the *cryD* gene is induced by light in the wild type, but not in mutants of the "white collar" gene *wcoA*. Targeted Δ*cryD* mutants show light-dependent phenotypic alterations, including changes in morphology and pigmentation, which disappear upon reintroduction of a wild-type *cryD* allele. In addition to microconidia, the colonies of the Δ*cryD* mutants produced under illumination and nitrogen starvation large septated spores called macroconidia, absent in wild-type colonies. The Δ*cryD* mutants accumulated similar amounts of carotenoids to the control strain under constant illumination, but produced much larger amounts of bikaverin under nitrogen starvation, indicating a repressing role for CryD in this biosynthetic pathway. Additionally, a moderate photoinduction of gibberellin production was exhibited by the wild type but not by the Δ*cryD* mutants. The phenotypic alterations of the Δ*cryD* mutants were only noticeable in the light, as expected from the low expression of *cryD* in the dark, but did not correlate with mRNA levels for structural genes of the bikaverin or gibberellin biosynthetic pathways, suggesting the participation of CryD in posttranscriptional regulatory mechanisms. This is the first report on the participation of a cry-DASH protein in the regulation of fungal secondary metabolism.

Filamentous fungi are a natural source for a large diversity of chemical compounds (1). Among them stand out many species of the genus *Fusarium*, a wide group of phytopathogenic fungi able to produce an extense array of metabolites and mycotoxins (2). A representative example is *Fusarium fujikuroi*, well known for its capacity to produce gibberellins (GAs), growth-promoting plant hormones with biotechnological applications (3). This fungus produces many other compounds (4), including pigments that provide characteristic colors to the mycelia. Under certain conditions, the *F. fujikuroi* cultures become reddish due to the synthesis of bikaverin, a polyketide pigment with antibiotic properties against protozoa and other organisms (5). When grown in the light, surface-grown mycelia acquire a characteristic orange pigmentation due to the synthesis of carotenoids, with the xanthophyll neurosporaxanthin as a major component (6). The enzymatic genes for the synthesis of GAs (reviewed in reference 7), bikaverin (8), and carotenoids (9) have been identified, and with the exception of some genes of the carotenoid pathway, they are organized in transcriptionally coregulated clusters.

Production of GAs, bikaverins, and carotenoids is modulated in *F. fujikuroi* by diverse environmental cues. Nitrogen availability is a major key regulatory signal in the control of secondary metabolism by this fungus, in which the three mentioned pathways are transcriptionally induced by nitrogen starvation (7, 8, 10). Considerable efforts have been devoted to identify the proteins involved in the regulation of GA and bikaverin biosynthesis. In the case of GA production, a central role is played by the transcription factor AreA, needed for the expression of the structural genes (7, 11, 12). AreA activity is modulated by ammonium availability, probably through the detection of its assimilation product, glutamine (13). Mutations of other genes involved in nitrogen assimilation, the glutamine synthetase gene *glnA* (14) and the major ammonium permease gene *mepB* (15), produce down- and upregulation of the GA genes, respectively, demonstrating their participation in the nitrogen regulatory mechanism. In contrast, bikaverin production is repressed by nitrogen in an AreA-independent manner, and it is modulated by other regulatory proteins, including those encoded by two genes present in the *bik* cluster (8). The biosynthesis requires acidic pH (16), indicating the participation of the pH regulatory protein PacC, whose deletion results in upregulation of the *bik* genes (8). Functional loss of the bZIP transcription factor MeaB results in a mild upregulation of the bikaverin genes in high nitrogen conditions, and this effect is significantly enhanced in the absence of AreA (17), reflecting the complexity of the regulatory network governing this pathway.

Light is an environmental signal widely used by fungi to modulate developmental and metabolic processes (18, 19). As indicated above, light induces the synthesis of carotenoids in *F. fujikuroi* (6), a response similar to that observed in other fungi, as *Neurospora crassa* (20) or *Phycomyces blakesleeanus* (21). Additionally, light stimulates gibberellin biosynthesis in some *F. fujikuroi* strains (9), but this response is of a lesser magnitude compared to photocarotenogenesis and has barely been investigated. In *N. crassa*, a well-known photobiology model, most photoresponses are mediated by the "white collar" (WC) complex (22), a heterodimer formed by the proteins WC-1 and WC-2 (23). Upon illumination, the WC complex binds upstream promoter sequences of light-regulated genes, including those of the carote-

Received 11 October 2012 Accepted 11 February 2013
Published ahead of print 15 February 2013
Address correspondence to Javier Avalos, avalos@us.es.
Supplemental material for this article may be found at http://dx.doi.org/10.1128/AEM.03110-12.

doi:10.1128/AEM.03110-12

noid pathway, to induce their transcription. The photoreception function in the complex is played by WC-1 through its LOV flavin-binding domain (24). Similar WC complexes were found to play diverse photoreception roles in other fungi (25). Contrary to what was expected, the mutants of the only WC-1-like gene of *F. fujikuroi*, *wcoA*, (26), or *Fusarium oxysporum*, *wc1* (27), conserved the photoinduction of the carotenoid pathway, pointing to the participation of a different photoreceptor system. However, the *wcoA* mutation led to unexpected changes in the production of different metabolites of *F. fujikuroi*, including a sharp decline in the production of GAs irrespective of light (26), preventing conclusions to be drawn about the possible role of the WcoA protein on GAs' photostimulation.

No information is available on the photoreceptors involved in the known *Fusarium* photoresponses. The analysis of the freely accessible *Fusarium* genomes reveals the presence of several genes for presumed photoreceptors. These include a DASH (for *Drosophila*, *Arabidopsis*, *Synechocystis*, human) cryptochrome (9) and a second cryptochrome gene related to plant cryptochromes, which is under investigation (P. Wiemann and B. Tudzysnki, unpublished data). Cryptochromes are blue/UV-A light photoreceptors which probably evolved from photolyases, enzymes able to use light as an energy source to repair UV-B-induced lesions (28, 29). Cryptochromes typically have a N-terminal photolyase-related domain able to bind two chromophores, flavin adenine dinucleotide (FAD) and 5,10-methenyltetrahydrofolate (MTHF) or pterin, followed by a long C-terminal domain absent in photolyases, reported to play regulatory roles related to light control of growth, development, cell signaling, and circadian rhythm in different taxonomic groups (28). The DASH cryptochromes (abbreviated hereafter as cry-DASH) are a subgroup in this family that differ from cryptochromes in the ability to repair single-stranded DNA (reviewed in reference 28) and the lack of the long carboxy extension. The unexpected role of WcoA on secondary metabolism (26) and the lack of knowledge on the functions of cryptochromes in fungi have led us to perform a functional analysis of the *F. fujikuroi* cry-DASH gene, which we called *cryD*. Expression of *cryD* was induced by light in the wild type (WT) but not in *wcoA* mutants, and lack of a functional *cryD* allele led to several light-dependent effects, such as morphological alterations, production of macroconidia under nitrogen starvation, and enhanced bikaverin biosynthesis. As formerly found with the *wcoA* mutation, the *cryD* mutants kept the induction of the synthesis of carotenoids in the light, but they did not exhibit photostimulation of GA production. Our results provide new insights into the biological functions of DASH cryptochromes in fungi, with the first example of a role in the regulation of secondary metabolism.

MATERIALS AND METHODS

***Fusarium* strains and culture conditions.** The FKMC1995 wild-type strain of *Fusarium fujikuroi* (*G. fujikuroi* mating population C) was obtained from the Kansas State University Collection (Manhattan, KS). The Δ*wcoA* mutants SF225 and SF226 correspond to the former M5 and M6 mutants (26). The carotenoid-overproducing strains (*carS* mutants) SF114, SF115, SF116, and SF134 have been described formerly (30). The transformants T1 and T3, described in this work, were renamed SF236 and SF237, according to the terminology of the *Fusarium* strain collection kept by the authors.

For growth, DG minimal medium (31) with 3 g liter^{-1} of L-asparagine instead of $NaNO_3$ as a nitrogen source (DGasn) was used. For phenotypic analyses, plates were incubated for 7 days at 22°C or 30°C as indicated, either under constant illumination (7 W m^{-2} white light obtained with a battery of four fluorescent lights) or under darkness. Illumination with red or blue light was obtained by filtration with commercial cellophane sheets. In this case, light intensities were 6 W m^{-2}, 1,5 W m^{-2}, and 1,7 W m^{-2} for white, blue, and red light, respectively. For carotenoid analysis, DGasn plates were incubated for 7 days at 30°C, either under constant white light illumination (7 W m^{-2}) or in the dark. For expression analyses of genes *carRA*, *carB*, *wcoA*, and *cryD*, 10^6 conidia of the indicated strain were pregerminated for 9 h in 0.1 ml of DGasn at 30°C, added to a 14-cm^2 petri dish with 80 ml of liquid DGasn medium, and incubated at 30°C for 3 days. For bikaverin and GA analyses and for expression analyses of *gib* and *bik* genes, strains were grown up to 7 days in a 500-ml Erlenmeyer flask with 250 ml liquid high-N medium (ICI medium [32]) or low-N medium (ICI medium with 10% of the nitrogen source). Each flask was inoculated with 10^6 fresh conidia and incubated in the dark or under 3 W m^{-2} white light in a rotary shaker at 200 rpm in a 30°C chamber.

Formation of microconidia and macroconidia was determined on mycelia grown on solid minimal medium (DGasn) and low-N minimal medium (low-N DGasn: DGasn with 0,625 g l^{-1} asparagine) at 22°C in the dark or under white light illumination (5 W m^{-2}).

For DNA extractions, the strains were incubated for 5 days at 30°C in 250-ml Erlenmeyer flasks with 100 ml of DGasn inoculated with 10^5 conidia.

Cloning of *cryD* and generation of Δ*cryD* mutants. To generate the Δ*cryD* mutants, a plasmid was constructed with a hygromycin resistance (Hyg^r) cassette, containing the *Escherichia coli* hygromycin phosphotransferase gene *hph* under the control of *Aspergillus nidulans* regulatory sequences. For this purpose, a 4.2-kb region containing the whole *cryD* gene was obtained by PCR with primer set 1 (Table 1) and cloned in pGEM-T (Promega, Mannheim, Germany). The resulting plasmid was used as the template for reverse PCR amplification with primer set 2. The resulting amplification product is the linearized vector lacking 1.3 kb in the 5′ region of the *cryD* gene. The deleted region was replaced with the Hyg^r cassette, obtained from plasmid pAN7-1 (33), resulting in plasmid pDCryD. Transformation of *F. fujikuroi* was done following Proctor et al. (34) by incubating 3×10^8 protoplasts of strain FKMC1995 obtained from 5×10^8 starting conidia with a mixture of 30 μg of plasmid pDCryD previously linearized with NotI and 10 μg of undigested plasmid. For selection, hygromycin (Roche, Mannheim, Germany) was added to the medium at a final concentration of 50 mg liter^{-1}. Hygromycin-resistant colonies appeared after 1 week of incubation.

For Southern blot analysis, genomic DNA from the wild type and three transformants was extracted as described previously (35) and digested with EcoRI, BamHI, or DraI. DNA was quantified using a Nanodrop ND-100 spectrophotometer (Nanodrop Technologies, Wilmington, DE), and the same amount of digested DNA was loaded per lane on a 0.8% agarose gel. After electrophoresis, DNA fragments were transferred to a Hybond N membrane (GE Healthcare, Little Chalfont, Buckinghamshire, United Kingdom). Primer set 3 was used to amplify a *cryD* 1.6-kb internal fragment by PCR. This product was digested with NcoI, and the resulting 1.3-kb fragment was used as a probe for hybridization with the membrane-bound fragments of genomic DNA (36). The probe was heated for 10 min at 100°C and incubated afterwards for 3 to 4 h at 37°C with 2 μl hexanucleotide mix (10×), 2 μl of a pool of nonradioactive dATP, dGTP, and dTTP (0.5 mM), 2 μl of [α-^{32}P]dCTP (3,000 Ci mmol^{-1}; Perkin-Elmer, Boston, MA), and 2 U of the Klenow fragment of *E. coli* DNA polymerase I. The labeled probe was purified with the GFX DNA purification kit (GE Healthcare).

To check the replacement of an internal region of the *cryD* gene by the Hyg^r cassette, genomic DNA samples from the investigated strains were used as the substrate for PCR amplifications. Primer set 4 was used to detect the *hph* gene (expected 1.02-kb product), and primer set 5 (forward primer 1.25 kb upstream of the *cryD* coding sequence; reverse primer from the *cryD* coding sequence, positioned 787 bp upstream of the stop

TABLE 1 Primers used in this work

Primer set	Application	Primer sequence	
		Forward	Reverse
1	*cryD* cloning	5′-TAGACCTGGACAAATCGGAG-3′	5′-CTGCTGGAACGGGGCTACAG-3′
2	*cryD* reverse PCR	5′-TAGACGAGGAGTTTATTCCCAGCC-3′	5′-CGGCTACACCTCGAACCGAG-3′
3	*cryD* probe	5′-TCTGACAGCGTCTCCGCC-3′	5′-CATTCAGCTCCGTAGCGC-3′
4	*hph* detection	5′-TGCCTGAACTCACCGCGACG-3′	5′-TATTCCTTTGCCCTCGGACG-3′
5	*cryD* detection (Fig. 3)	5′-TAGACCTGGACAAATCGGAG-3′	5′-CATTCAGCTCCGTAGCGC-3′
6	*cryD* complementation	5′-CACGGGATATCTGGCCAGGA-3′	5′-TTTCGAGATATCCGCAAAGGAG-3′
7	*cryD* detection (Fig. 6)	5′-GCTTGTTCCCCATCCATCTA-3′	5′-GAAAGACAGGAGGAAGATGG-3′
8	*cryD* detection (Fig. 6)	5′-GCTTGTTCCCCATCCATCTA-3′	5′-AGGGTTGAAGATGCGTGCGT-3′
9	*nptII* detection	5′-GAACAAGATGGATTGCACGC-3′	5′-CGCTCAGAAGAACTCGTCAA-3′
10	*cryD* cDNA detection	5′-CAGAAGCTGTTCCCGAAGACA-3′	5′-AGGGTTGAAGATGCGTGCGT-3′
11	RT-PCR, *wcoA*	5′-TGAGATTGTCGGCCAGAATTG-3′	5′-GAGCCCGCTTCGACTTTG-3′
12	RT-PCR, *carRA*	5′-CGGGACTACATGCGATTGTG-3′	5′-CTTGAAAAGACGTGAGCCAAA-3′
13	RT-PCR, *carB*	5′-TCGGTGTCGAGTACCGTCTCT-3′	5′-TGCCTTGCCGGTTGCTT-3′
14	RT-PCR, *cryD*	5′-CAGAAGCTGTTCCCGAAGACA-3′	5′-TGCGATGCCCATTTCTTGA-3′
15	RT-PCR, *bik1*	5′-CTCGTCACCGACGCTCTAGTC-3′	5′-TGGGCATTGACCGGTATCA-3′
16	RT-PCR, *bik2*	5′-CGAAGCTAGGCTCGGGAAGT-3′	5′-CAACAAGAACACCACCACATTGA-3′
17	RT-PCR, *bik3*	5′-GGCCGAAGATATCCGAATTTT-3′	5′-CCTCCGATTTCTGCGTGTTT-3′
18	RT-PCR, *gibB*	5′-TGTCAGCGAATCTGCTCCAA-3′	5′-GACGCATAACGGATGAAATGAG-3′
19	RT-PCR, *gibD*	5′-GCCTTCCGTGCAGTAGAAGAA-3′	5′-GGCATGAACCACTGGACTACAG-3′
20	RT-PCR, *gibG*	5′-GCTCGCCCCTCCTTATCC-3′	5′-TGGCTTCCCTTTCCTTGCT-3′
21	RT-PCR, β-tubulin	5′-CCGGTGCTGGAAACAACTG-3′	5′-CGAGGACCTGGTCGACAAGT-3′

codon) was used to detect the *cryD* gene (2.7-kb product expected for the wild-type allele and 5.3-kb product for the mutant allele).

Complementation of the Δ*cryD* mutation. The wild-type *cryD* gene, including 680 bp and 870 bp of upstream and downstream regulatory sequences, was amplified from FKMC1995 genomic DNA with primer set 6 and cloned in pGEM-T. The gene was removed from the resulting plasmid by EcoRI digestion and cloned into the EcoRI site of pNTP2 (kindly provided by Attila Ádám), to yield plasmid pCcryD. pNTP2 is a 4.8-kb plasmid containing the neomycin phosphotransferase II gene (*nptII*) fused to cauliflower mosaic virus 35S promoter and terminator sequences. For complementation, 40 μg of pCcryD was used to transform 3×10^8 protoplasts of the Δ*cryD* mutant SF236. For selection, Geneticin (G418 disulfate salt; Sigma-Aldrich, St. Louis, MO) was added to the medium at a final concentration of 150 mg liter^{-1}. Genomic DNA samples were obtained from the transformants and used to check by PCR the occurrence of the *hph* gene (primer set 4), the *nptII* gene (primer set 9), and total or partial sequences of the *cryD* gene (primer sets 7 and 8, respectively).

Gene expression. For expression analyses of genes *carRA*, *carB*, and *cryD*, quantitative reverse transcription-PCR (qRT-PCR) analyses were performed with total RNA samples obtained from 3-day-old cultures grown at 30°C in the dark in DGasn medium. To determine the effect of light on mRNA levels of genes *wcoA* and *cryD* in the wild type, the dark-grown 3-day-old cultures were exposed to 5 W m^{-2} white light for 15, 30, 60, 120, and 240 min. For expression analysis of *bik* and *gib* genes in the wild type and Δ*cryD* mutants, mycelial samples were collected from each high-N or low-N flask after 2, 4, and 7 days of incubation, separated from the medium by filtration, dried on filter paper, frozen in liquid nitrogen, and stored at −80°C. RNA was extracted from the samples with the RNeasy plant minikit (Qiagen, Chatsworth, CA), and its concentration was estimated with a Nanodrop ND-100 spectrophotometer. For cDNA synthesis, the Transcriptor first-strand cDNA synthesis kit (Roche, Mannheim, Germany) was used, and concentrations were set to 25 ng μl^{-1} in every sample. qRT-PCR analyses were performed in a LightCycler 480 real-time instrument (Roche) with the LightCycler 480 SYBR green I Master (Roche), using primer sets 11 to 20 (Table 1), corresponding to the genes *wcoA*, *cryD*, *bik1*, *bik2*, and *bik3*. The β-tubulin gene (primer set 21) was used as the control for constitutive expression. mRNA values of each condition and strain were normalized against the β-tubulin transcript level and referred to the value of the wild type before light exposure or to the wild-type 2-day dark-grown culture value for *bik* and *gib* expression.

To confirm complementation of the Δ*cryD* mutants, occurrence of wild-type *cryD* transcript was assayed by PCR amplification with primer set 10 (Table 1) on cDNA samples from 3-day-old mycelia of the transformants incubated for 60 min under white light.

Chemical analyses. Carotenoids were extracted from freeze-dried samples with acetone in a FastPrep-24 device (MP Biomedicals, Irvine, CA) as described by Arrach et al. (37). Samples were dried and resuspended in hexane for spectrophotometric measurements. Total amounts of carotenoids were estimated from maximal absorption spectra, assuming an average maximal E (1 mg liter^{-1}, 1 cm) of 200. All of the values were corrected according to the dry weight and dilution of the sample.

Samples for bikaverin determinations were obtained from filtered 7-day-old submerged cultures. Bikaverin pigments were extracted with acetone from mycelia through cell breakage in a Fast-Prep-24 device and precipitated with 10 N NaOH (26). For secreted bikaverin analyses, filtrate samples were acidified to pH 2.5 with 1 N HCl and extracted with chloroform. Both types of samples were analyzed spectrophotometrically in chloroform, and total amounts were estimated from absorbance at 521 nm (38).

Gibberellins (GAs) were extracted from 0.5 ml of acidified filtered medium and run in parallel to a GA3 standard on thin-layer chromatography (TLC) as described previously (39). The samples were dried, dissolved in 6 μl acetonitrile, loaded on silica gel 60 TLC plastic sheets (Merck, Darmstadt, Germany), and run in benzene–*n*-butyl alcohol–acetic acid (60:30:10) as the mobile phase. For GA visualization and quantification, the TLC sheets were sprayed with a mixture of ethanol and sulfuric acid and visualized as described by García-Martínez et al. (40). Relative GA3 production was estimated by densitometry analysis with the ImageJ 1.42q program (Wayne Rasband, NIH, Bethesda, MD; http://rsb.info.nih.gov/ij).

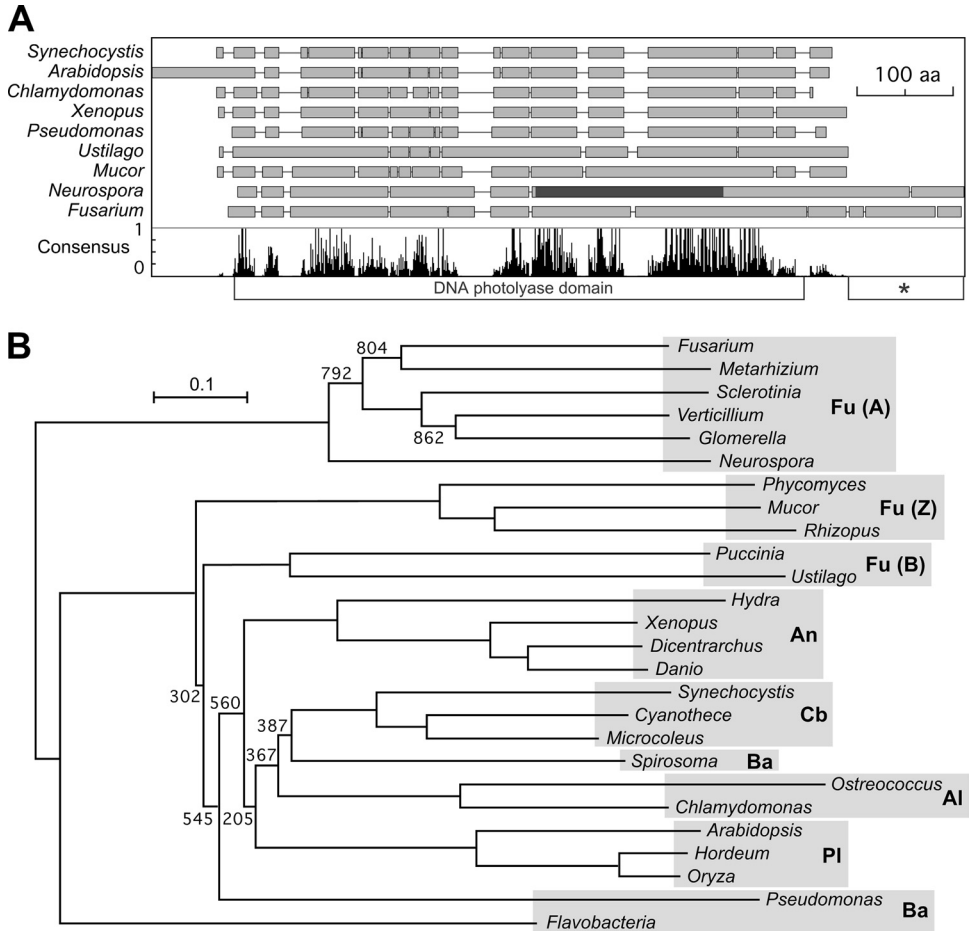

FIG 1 Sequence analysis of cry-DASH proteins. (A) Simplified representation of the Clustal comparison between cry-DASH proteins from *F. verticillioides* and eight species from representative taxonomic groups. Breaks between the boxes represent gaps introduced by the Clustal program to facilitate alignment. The diagram below plots the presence of the consensus amino acids as given by the Clustal analysis. The photolyase domain is represented below the plot. The dark segment in the *Neurospora* protein indicates the region containing residues involved in FAD binding (data according to Froehlich et al. [51]). The asterisk indicates the carboxy extension displayed in Fig. S2 in the supplemental material. (B) Neighbor-joining phylogram of 26 representative cry-DASH proteins. Reliability of clusters was evaluated by bootstrapping with 1,000 replicates (bootstrap values are indicated). Genus names stand for the following species (with protein accession numbers given in parentheses: *Fusarium verticillioides* (FVEG_02442), *Metarhizium anisopliae* (EFZ01174), *Sclerotinia sclerotium* (SS1G_05163), *Verticillium albo-atrum* (VDBG_00705), *Glomerella graminicola* (EFQ26657), *Neurospora crassa* (NCU00582), *Phycomyces blakesleeanus* (85761), *Mucor circinelloides* (156465), *Rhizopus oryzae* (RO3G_16297), *Puccinia graminis* (XP_003326630), *Ustilago maydis* (EAK86731), *Hydra magnipapillata* (XP_002166544), *Xenopus laevis* (NP_001084438), *Dicentrarchus labrax* (CBN81995), *Danio rerio* (NP_991249), *Synechocystis* sp. (P77967), *Cyanothece* sp. (YP_002375679), *Microcoleus chthonoplastes* (ZP_05026729), *Spirosoma linguale* (YP_003390944), *Ostreococcus tauri* (Q5IFN2), *Chlamydomonas reinhardtii* (XP_001701871), *Arabidopsis thaliana* (Q84KJ5), *Hordeum vulgare* (BAK06380), *Oryza sativa* (NP_001058278), *Pseudomonas fulva* (YP_004472278), and *Flavobacteria* bacterium (ZP_03701378). The shaded areas group the species by taxonomic categories. The abbreviations on the right represent fungi (Fu; in which ascomycetes [A], basidiomycetes [B], and zygomycetes [Z] are distinguished), cyanobacteria (Cb), bacteria (Ba), algae (Al), animals (An), and plants (Pl).

Conidiation assays. For conidiation analyses, 7 colonies were grown on and low-N DGasn media. After 7 days, conidia were collected and microconidia and macroconidia were quantified in a hemocytometer (41). Pictures were taken from concentrated samples in a Leica DM1000 microscope. Conidial determinations are the results of three independent experiments.

Protein sequence analyses. Protein alignments were achieved with the ClustalX 1.83 program (42). Protein domains were determined with the SMART architecture research online tool (http://smart.embl.de/) (43). Accession numbers for the *F. verticillioides*, *F. oxysporum*, and *F. graminearum* proteins are the codes for the respective annotated proteins in the *Fusarium* comparative database (http://www.broadinstitute.org/annotation/genome/fusarium_group/MultiHome.html). Accession number 156465, for *Mucor circinelloides*, is the code for the corresponding annotated protein in the genome database for this fungus (http://genome.jgi-psf.org/Mucci2/Mucci2.home.html).

Nucleotide sequence accession number. The cry-DASH protein sequence for *Fusarium fujikuroi* has been submitted to EMBL under accession no. HE650104.

RESULTS

Sequence analysis of fungal cry-DASH genes. Genes encoding putative cry-DASHs are found in different taxonomic groups, from filamentous fungi to animals, plants, algae, bacteria, and archaea. The analysis of the three publicly available *Fusarium* genome databases indicated the occurrence of a single cry-DASH-encoding gene in this genus, which we named *cryD*. A Clustal comparison of the predicted CryD from *Fusarium verticillioides* with representative cry-DASHs from different origins showed the conservation of the characteristic photolyase domain (Fig. 1A). Irrespective of this overall domain structure, different cry-DASH

sequence patterns were observed, with evident divergences between the various considered fungal taxonomic groups, ascomycetes, basidiomycetes, and zygomycetes. These differences were further supported by a phylogenetic analysis of these and other cry-DASHs from different phyla. The tree displayed in Fig. 1B shows that cry-DASHs from ascomycete fungi differ in their phylogenetic origin from those of other taxonomic groups, including the basidiomycete and zygomycete fungi (see Fig. S1 in the supplemental material for more detailed analysis of *Fusarium* and ascomycete cry-DASH sequences). This difference would be compatible either with a single ancestral separation or with an independent origin of ascomycete cry-DASHs from those found in other species.

Comparison of fungal cry-DASHs showed the occurrence of a carboxy-terminal extension in ascomycetes, mostly absent in the analyzed cry-DASHs from other fungal phyla. Comparison of eight of such extensions from different ascomycetes revealed that they are variable in sequence and length, from 44 to 115 amino acids (aa) in the cases investigated compared to those of the *Mucor circinelloides* (156465) and *Ustilago maydis* (UM05917) orthologues. These extensions showed low sequence conservation, except for a preference for glycine in several positions (see Fig. S2 in the supplemental material).

Identification and expression of the *F. fujikuroi cryD* gene. The predicted proteins encoded by the *cryD* genes of *F. verticillioides* (FVEG_02442) and *F. oxysporum* (FOXG_03570) show a high degree of identity (94%), but that encoded by the orthologous gene in *Fusarium graminearum* (FGSG_08852) exhibits an unexpectedly high degree of divergence (68% conserved positions along its 678 aa compared to the 715 aa of FVEG_02442 and FOXG_03570). Based on the high sequence conservation between the two cry-DASH genes and the 5′ and 3′ neighbor genes in *F. verticillioides* and *F. oxysporum*, two primer sets were designed from sequence alignments and used to amplify by PCR 1.60- and 1.28-kb products of *F. fujikuroi* DNA, located upstream and downstream of the *cryD* coding sequence, respectively. Once their sequence analyses confirmed the cloning of the correct DNA segments, two new primers were designed to amplify by PCR and clone the *cryD* coding sequence. Assembly of the obtained sequences led to the definition of the whole *F. fujikuroi cryD* gene sequence, including upstream and downstream noncoding sequences, which was deposited in the EMBL gene database. As expected, the *F. fujikuroi cryD* gene was highly similar to those of *F. verticillioides* and *F. oxysporum*, with that of *F. verticillioides* as its closest relative (93.5% and 95% identity at coding DNA and protein sequence, respectively [see Fig. S3 in the supplemental material]).

The availability of the *cryD* sequence allowed the design of primers for qRT-PCR expression analyses. In contrast to the lack of significant light induction formerly reported for the white collar gene *wcoA* (26), the *cryD* mRNA levels increased rapidly following illumination, reaching nearly 100-fold induction after 1 h of light treatment and declining slowly afterwards (Fig. 2A). In contrast, no significant *cryD* photoinduction was recognized in Δ*wcoA* mutants, pointing to WcoA as a key photoreceptor in *cryD* photoregulation. Furthermore, *cryD* mRNA levels in the dark were about 10-fold lower in the Δ*wcoA* mutants than in the wild type, indicating a more general role of WcoA as a positive regulator of *cryD* expression.

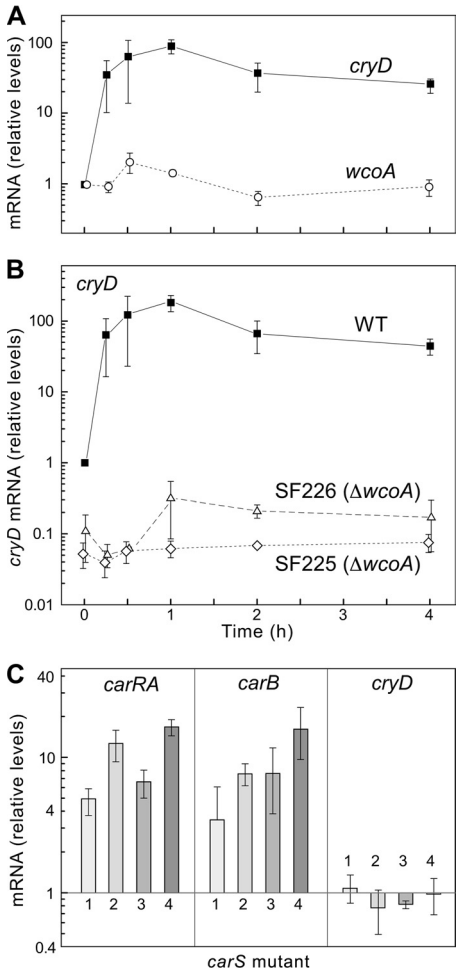

FIG 2 Expression of the *cryD* gene. (A) Effect of light on *cryD* and *wcoA* mRNA levels in wild-type *F. fujikuroi*. The data show qRT-PCR analyses of total RNA samples from the wild type grown in the dark or exposed for 15 min, 30 min, 1 h, 2 h, or 4 h to 7 W m^{-2} white light. Relative levels are referred to the values for each gene in the dark. All data show means and standard deviations for three measurements from three independent experiments. (B) Relative levels of mRNAs for genes *carRA* and *carB* in four carotenoid-overproducing mutants (*carS*) grown in the dark, numbered 1 to 4 (1, SF114; 2, SF115; 3, SF116; and 4, SF134). The mRNA levels were referred to those of the wild type under the same conditions (C).

The *cryD* photoinduction resembled that of the genes coding for enzymes in the carotenoid pathway, such as *carRA* or *carB* (26, 44). These genes are also upregulated in the dark in *carS* carotenoid-overproducing mutants (30, 41). However, four independent *carS* mutants contained similar *cryD* mRNA levels in the dark to those of the wild type (Fig. 2B), indicating that *cryD* gene expression is not under the control of the CarS-mediated repressing mechanism.

Generation of Δ*cryD* mutants. The 1.60-kb and 1.28-kb DNA segments that included sequences upstream and downstream of the *cryD* coding region were used to construct a *cryD* deletion plasmid in which 1.3 kb of the *cryD* coding sequence was replaced by a Hyg^r cassette (Fig. 3A). Incubation of wild-type *F. fujikuroi* protoplasts with this plasmid led to the isolation of five transformants, denominated T1 to T5, which were subcultured from uninucleate microconidia under selective conditions to ensure

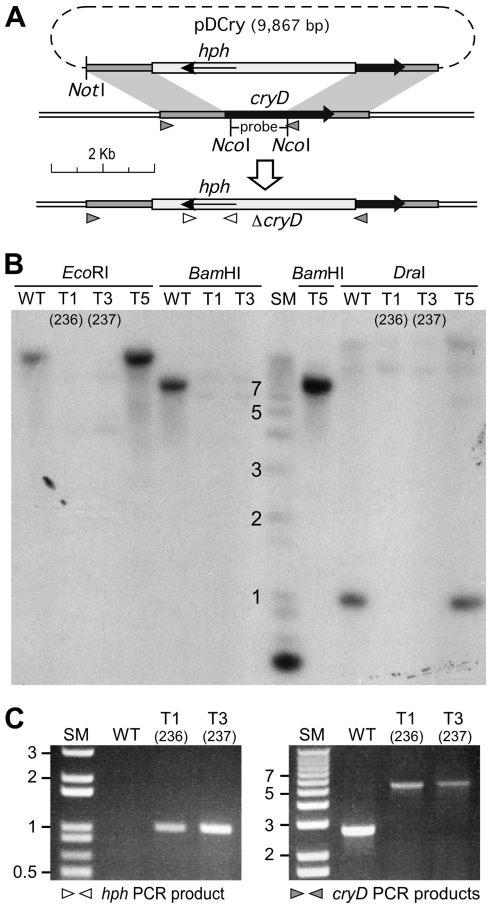

FIG 3 Generation of targeted Δ*cryD* mutants. (A) Schematic representation of the gene replacement event leading to the generation of Hyg^r Δ*cryD* transformants. The black arrow represents the *cryD* coding sequence. Plasmid pDCry contains the Hyg^r cassette with the *hph* gene (pale gray box) surrounded by upstream and downstream *cryD* sequences. The recombination events leading to *cryD* disruption occur in the shaded DNA segments, and the resulting physical map in the generated Δ*cryD* mutants is displayed below. The NotI and NcoI restriction sites used to linearize pDCry and to obtain the probe for the Southern blot, respectively, are indicated. (B) Southern blot of genomic DNA from the wild type (WT) and transformants T1, T3, and T5 digested with the indicated restriction enzymes and hybridized with the *cryD* probe indicated above. SM, size markers (relevant sizes in kb are shown). (C) Agarose gel electrophoresis of PCR amplification products obtained from DNA samples from the wild type and transformants T1 and T3 with the primer sets indicated below (see primer locations on panel A). (Left) Result with the *hph* primer set (Hyg^r; primer set 4 in Table 1). The expected PCR product (1 kb) indicates the presence of the *hph* gene. (Right) Result with the *cryD* primer set for sequences surrounding the deleted DNA segment in plasmid pDCry (primer set 5 in Table 1). The analysis allows detection of the correct gene replacement event. The wild-type allele gives a band of 2.7 kb, while the Hyg^r replacement results in a 5.3-kb PCR product. Lack of the 2.7-kb band in T1 and T3 confirms this replacement. These transformants were renamed SF236 and SF237.

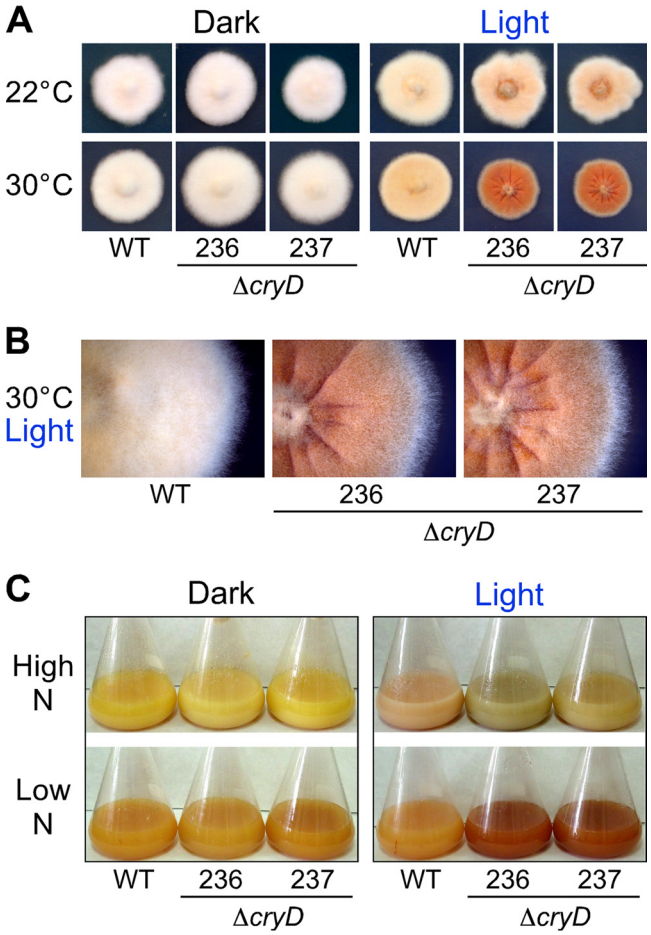

FIG 4 Visual phenotype of Δ*cryD* mutants. (A) Colonies of the wild type and Δ*cryD* mutants SF236 and SF237 (abbreviated 236 and 237, respectively) grown for 7 days at 22°C or 30°C on minimal medium in the dark or under constant illumination (7 W m^{-2}). (B) Partial magnification of the colonies grown in the light at 30°C. (C) Representative shake cultures of the wild type and the Δ*cryD* mutants SF236 and SF237 grown for 7 days at 30°C in high-nitrogen or low-N media in the dark or under constant illumination (3 W m^{-2}).

homokaryosis. Two of them, T1 and T3, exhibited a different phenotype from the wild type when grown at 30°C under light but not in the dark (Fig. 4A). Accordingly, they were suspected to have undergone a replacement of the wild-type *cryD* gene. To check the occurrence of the wild-type *cryD* allele, genomic DNAs of the wild type, T1, T3, and one of the transformants exhibiting a wild-type phenotype, T5, were digested with different restriction enzymes and hybridized by Southern blotting with the *cryD* DNA segment absent in the deletion plasmid. The film showed clear signals in the wild type and in T5, but no signals in T1 and T3 (Fig. 3B). PCR analyses confirmed the presence of the Hyg^r cassette and the replacement of the wild-type *cryD* gene in the transformants T1 and T3 (Fig. 3C). The latter is shown by the size of the PCR product obtained with DNA from transformants T1 and T3 with primer set 5 (Table 1; see the gray triangles in Fig. 3A and the result in the right graph of Fig. 3C), which coincides with the 5.4-kb size expected from the replacement. We conclude that T1 and T3 lack a functional *cryD* gene and therefore were subjected to a detailed phenotypic analysis. They are referred to hereafter as Δ*cryD* mutants SF236 and SF237.

Developmental phenotype of Δ*cryD* mutants. The colonies of the Δ*cryD* mutants exhibited the same appearance as the wild type in the dark, but differences in morphology and pigmentation were seen under constant illumination (Fig. 4A). The differences were more pronounced at 30°C than at 22°C: at the higher temperature, the mutants were deeply pigmented and exhibited a rougher surface and marked morphological alterations (Fig. 4B). In contrast

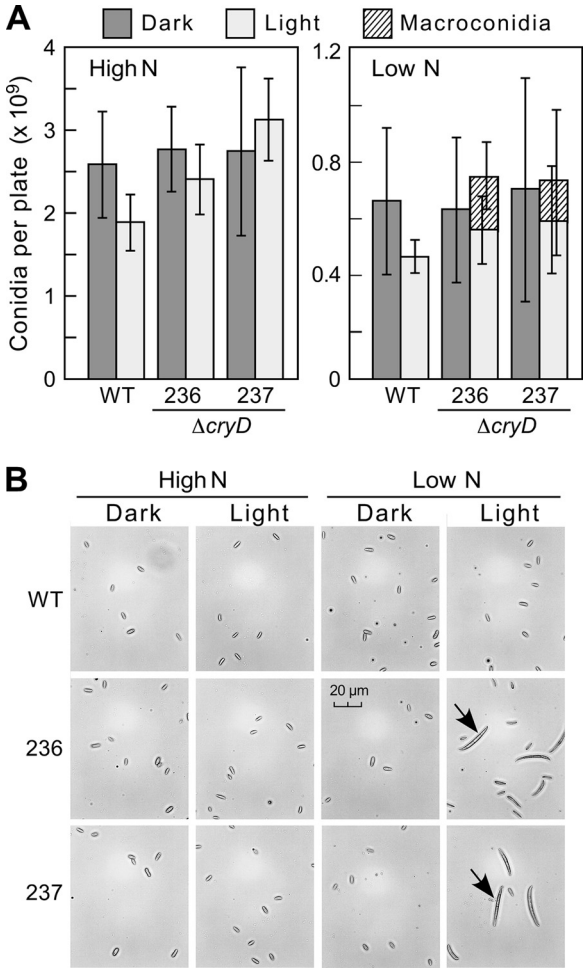

FIG 5 Effect of the Δ*cryD* mutation on conidiation. (A) Numbers of conidia produced by the wild type and the Δ*cryD* mutants SF236 and SF237 grown for 7 days under white light (7 W m^{-2}) in DGasn and DGasn low-N medium ("High N" and "Low N" on the graph, respectively). The data show averages and standard deviations from six biological replicates. (B) Conidium samples from representative examples of the data shown above. The pictures were taken under a microscope at 400×.

to the *wcoA* gene mutants (26), no apparent difference was detected in surface hydrophobicity of Δ*cryD* mycelia upon water addition, and the amounts of microconidia (small ellipsoidal uninucleated spores) were similar to those produced by the wild type (Fig. 5A). As formerly found (26), conidiation was not induced by light in any of the strains tested, either in DGasn or low-N DGasn medium (Fig. 5A, left panel).

As typically found in *F. fujikuroi* cultures, microconidia were the only class of spores found in most of the samples. However, macroconidia, long falciform septated cells, were also observed in the spore preparations from Δ*cryD* mutant colonies grown under nitrogen-limiting conditions in the light (Fig. 5B and right panel in Fig. 5A). Interestingly, no macroconidia were detected under any other tested conditions, including submerged cultures of the wild type or the mutants, irrespective of light or nitrogen availability. Formation of macroconidia is a widespread trait in other *Fusarium* species (45). This result suggests that CryD acts in *F. fujikuroi* as a nitrogen-dependent repressor of macroconidiation in surface cultures under illumination.

Effect of the Δ*cryD* mutation on pigment production. The mycelia of either the wild type or the Δ*cryD* mutants were weakly pigmented in the dark and contained small amounts of carotenoids. As expected, the wild type acquired a pale orange pigmentation when grown under constant illumination (Fig. 4A), which was accompanied by a 10-fold increase in the carotenoid content (see Fig. S4 in the supplemental material). Despite the visible differences in pigmentation compared to the wild type, the Δ*cryD* mutants exhibited the same increase in carotenoid content (see Fig. S4), indicating that carotenoid photoinduction is not prevented by the absence of a functional CryD cryptochrome. Therefore, the reddish pigmentation of the Δ*cryD* mutants in the light must be attributed to the accumulation of carotenoid-unrelated pigments, which are absent in the wild type.

Complementation of the Δ*cryD* mutation. To confirm that the alterations in pigmentation and morphology are produced by the loss of a functional *cryD* gene, the mutant SF236 was transformed with a plasmid with a wild-type *cryD* allele. Since SF236 contains the *hph* gene, a Geneticin resistance gene (*nptII*) was used in this case as a selective marker. After incubation of the protoplasts with the plasmid, six Geneticin-resistant colonies were obtained. Upon subculture from uninucleate microconidia, the six transformants were subjected to molecular and phenotypic characterization. PCR experiments (Fig. 6A) confirmed the presence of the *hph* gene in all the strains, except in the wild type, and the *nptII* gene in the six SF236-derived transformants, called here C1 to C6 (Fig. 6B). As expected, the SF236 Δ*cryD* mutant did not contain the entire *cryD* sequence (3.3-kb PCR product) or its 5′ region (2.1-kb product), found in the wild type. These *cryD* sequences were detected in transformants C1, C2, C3, C5, and C6, but not in C4. The absence of the 5′ *cryD* sequence in C4 suggests the disruption of the gene by ectopic integration of the plasmid through this DNA region. Expression of the *cryD* gene in C1, C2, C3, C5, and C6, but not in C4, was confirmed by PCR amplification of an internal *cryD* segment on cDNA samples from illuminated mycelia and by RT-PCR analyses (data displayed in Fig. S5 in the supplemental material).

The morphology and pigmentation of the colonies of transformants C1, C2, C3, C5, and C6 were similar to those of the wild type under white light. (C5 and C6 are shown in Fig. 6E; C1, C2, and C3 are shown in Fig. S5 in the supplemental material). However, transformant C4 conserved the characteristic phenotypic alterations of the Δ*cryD* mutants (Fig. 6E). The same result was obtained upon illumination with blue light, but not with red light, under which the Δ*cryD* mutants showed no major phenotypic changes. This result contrasts with the exhibition of a clear mutant phenotype by the Δ*wcoA* strain under red light (Fig. 6E). Taken together, the results strongly support that the loss of a functional *cryD* gene is responsible for the phenotypic alterations exhibited by the Δ*cryD* mutants and that this effect requires the participation of a blue-light photoreceptor.

Effect of the Δ*cryD* mutation on bikaverin production. As already mentioned, bikaverin is a well-known reddish secondary metabolite produced by this fungus (Fig. 7A). To check the possible role of CryD in the production of this pigment, the wild type and the Δ*cryD* mutant strains were grown in high-N and low-N media, in the dark or under constant illumination. Under these culture conditions, the illuminated cultures of the Δ*cryD* mutants exhibited a different hue in high-nitrogen medium and a deep reddish color in low-N medium, not apparent in the wild type

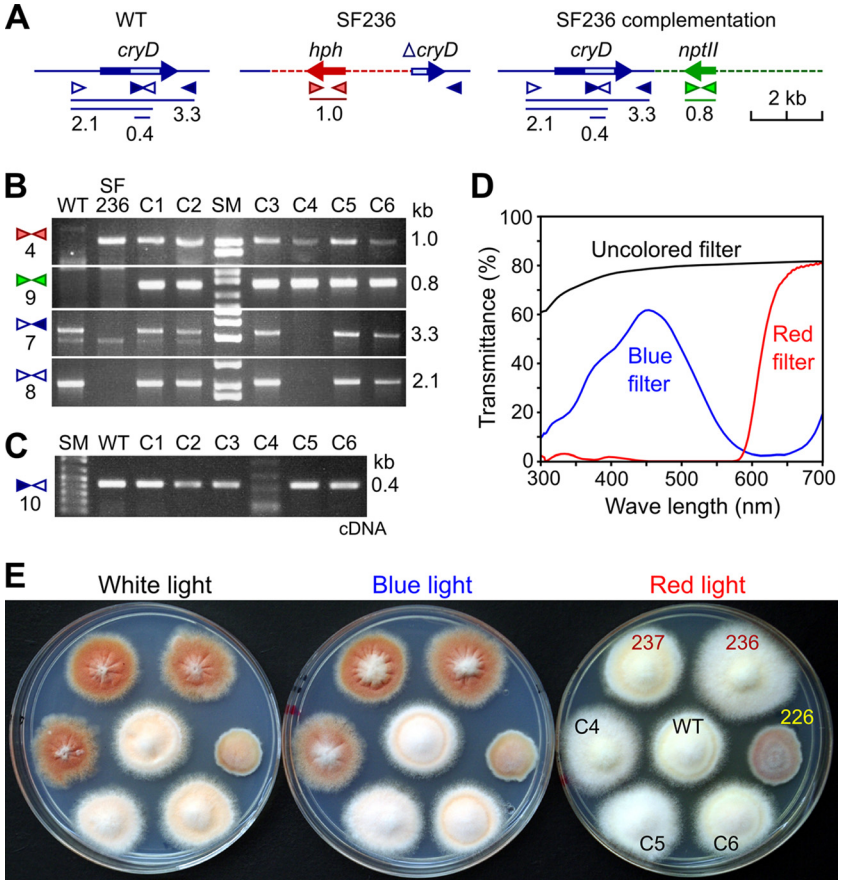

FIG 6 Complementation of the Δ*cryD* phenotype. (A) Schematic representation of primer locations and PCR products (sizes in kb) for the *cryD* gene in the wild type (WT), the *hph*-disrupted allele in the Δ*cryD* mutant SF236, and the construct added to SF236 in the transformation experiment. The light box in the *cryD* gene represents the predicted FAD binding domain. (B) Agarose gel electrophoresis of PCR amplification products obtained from genomic DNA samples of the wild type (WT), the Δ*cryD* mutant SF236, and the SF336-derived transformants C1 to C6. Primer sets are numbered on the left according to Table 1. Expected PCR products are indicated on the right. The 1-kb band (primer set 4) and the 0.8-kb band (primer set 9) indicate the presence of the *hph* and *nptII* genes, respectively. The 2.1- and 3.2-kb bands indicate the presence of the 5′ *cryD* sequence or the entire *cryD* sequence, respectively. (C) Agarose gel electrophoresis of the PCR amplification products obtained with primer set 10 from cDNA samples of the wild type (WT) and the complementation transformants C1 to C6 after 1 h of exposure to light. The 0.4-kb product indicates the presence of *cryD* transcript. (D) Transmittance spectra of cellophane sheets used as filters for illumination with white light (uncolored filter), blue light (blue filter), and red light (red filter). (E) Visual phenotype of the wild type (WT), the Δ*cryD* mutants SF236 and SF237, the Δ*wcoA* mutant SF226, and the transformants C4, C5, and C6 grown upon illumination with white, blue, or red light (see transmittance spectra).

(Fig. 4C). The reddish pigments extracted from these strains showed the typical bikaverin absorption spectrum, with a maximum at 521 nm (Fig. 7B). Bikaverin concentrations were determined for all the tested culture conditions, either in the mycelium or in the culture filtrates. Bikaverin was also found in small amounts in the cultures in high-nitrogen medium, where its color was likely masked by other pigments (Fig. 4C). However, the bikaverin levels were significantly enhanced in the mycelia of the Δ*cryD* strains upon illumination (Fig. 7C). This effect was particularly outstanding in low-N medium, where the illuminated cultures of the mutants accumulated much larger amounts of bikaverin either in the mycelium or in the medium. No relevant differences were observed, however, in the dark, indicating a light-dependent role of CryD in the nitrogen regulation of bikaverin biosynthesis.

To check if the Δ*cryD* mutation exerts its effect on gene expression of enzymatic genes for the bikaverin pathway, qRT-PCR analyses were achieved to determine transcript levels in the wild type and Δ*cryD* mutants after 2, 4, and 7 days of incubation in low-N medium. In agreement with former results (8), mRNA levels for the polyketide synthetase gene *bik1* (*pks4*) (46) showed a tendency to increase in the wild type during incubation in this medium, but the mRNA pattern was not affected by light. A similar tendency was exhibited by *bik3* in the dark but not by *bik2*, although a minor light induction was apparent for both genes in this case. The results were very similar in the Δ*cryD* mutants, except that a propensity for larger mRNA amounts was apparent in most cases. Overall, the differences in *bik1*, *bik2*, *and bik3* mRNA levels between the wild type and *cryD* mutants were too minor to explain the large differences in bikaverin production, suggesting the participation of CryD in a nontranscriptional regulatory mechanism.

Effect of the Δ*cryD* mutation on gibberellin production. Because of their similar nitrogen regulation, the effect of the Δ*cryD* mutation on bikaverin biosynthesis led us to investigate its effect on GA production in the same experiments. The filtrates of the

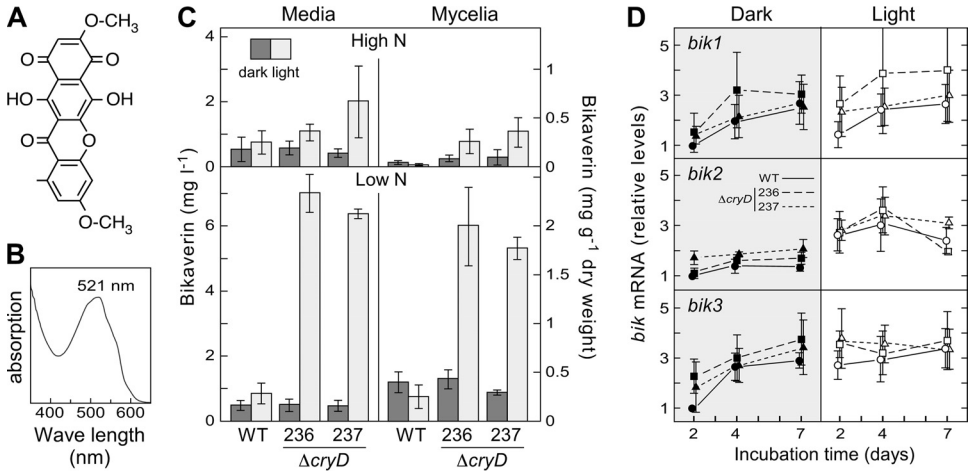

FIG 7 Effect of the Δ*cryD* mutation on bikaverin production. (A) Chemical structure of bikaverin. (B) Representative example of absorption spectrum of the red pigment isolated from the shake cultures of the Δ*cryD* mutants SF236 and SF237 grown in low-N medium in the light (Fig. 4C). (C) Bikaverin concentrations in the mycelia and the filtrates of shake cultures of the same strains grown for 7 days at 30°C in high-N or low-N media in the dark or under constant illumination (3 W m^{-2}). (D) qRT-PCR analyses for genes *bik1*, *bik2*, and *bik3* in RNA samples from the mycelia of cultures after 2, 4, and 7 days of incubation in low-N medium. Relative expression was referred to the value of the wild type in the dark. The data on bikaverin and *bik* mRNA levels show averages and standard errors from three independent experiments.

wild-type and Δ*cryD* cultures contained similar amounts of gibberellic acid in the dark, but a ca. 40% increase was found in those of the wild type when grown under light (Fig. 8A). However, this light induction was not apparent in the cultures of the Δ*cryD* mutants.

The light-induced increase in the GA content of the wild-type cultures was too limited to expect significant changes in expression of the structural genes of the gibberellin pathway. However, the mRNA levels for three GA genes were analyzed in the same RNA samples described in the experiments in Fig. 7D. The genes chosen for this assay were *gibB*, coding for *ent*-kaurene synthase or *ent*-copalyl diphosphate synthase, in turn the first specific enzyme of GA biosynthesis, *gibD*, coding for the P450-1 enzyme, and *gibG*, coding for the desaturase responsible of the last reaction of the pathway. These three genes were originally called *cps*/*ks*, *P450-1*, and *des*, respectively (7). As expected, the mRNA content for the three genes was low in the early stage of the cultures (2 days) and augmented in later stages (4 and 7 days) (Fig. 8B), when nitrogen is exhausted (47). However, in contrast to the GA3 amounts found in the cultures, mRNA contents in the wild type reached higher levels in the dark than under illumination, suggesting that CryD facilitates a more efficient translation of *gib* transcripts in the light, possibly linked to enhanced mRNA degradation. Interestingly, the Δ*cryD* mutants exhibited a delayed time course of mRNA accumulation for the three genes compared to the wild type, suggesting also the implication of CryD in the rapid response to nitrogen starvation.

DISCUSSION

Cryptochromes were defined as photolyase-like proteins with no DNA repair activity but with known or presumed blue-light photoreceptor functions (28, 48). The functional diversity of these photoreceptors became more evident when new members of this protein family were described in recent years, and cryptochromes are currently divided into at least seven subfamilies (49). One of the subfamilies comprises the cry-DASHs (50), widespread in photosynthetic organisms, but also found in some nonphotosynthetic bacteria, archaea, animals, and fungi. In the latter, genes for cry-DASHs have been found in ascomycete, basidiomycete, and zygomycete genomes. Our analyses showed high sequence divergence between cry-DASHs of the three fungal groups, indicating distant evolutionary origins. The difference is further emphasized by a carboxy-terminal extension usually found in cry-DASHs of ascomycetes, but rarely present in those of basidiomycetes and zygomycetes or other phyla compared in our analyses. Whether these extensions play a specific biological role needs to be addressed in future studies.

The functions of two ascomycete cry-DASH proteins were recently investigated *in vivo* through the generation of targeted mutations: *cry* in *N. crassa* (51) and *cry1* in *Sclerotinia sclerotiorum* (52). In *N. crassa*, the white collar system centralizes the light detection of all of its known photoresponses (53). Hence, the role of the genes for other putative photoreceptors found in its genome, including one for a cry-DASH, remains a challenging task. The mutations of some of them result in weak light-related phenotypic effects, but in most cases there is no apparent change in any light-controlled phenomenon (53). In the case of the cry-DASH gene of *N. crassa*, the mutation caused no phenotypic alterations except a slight but detectable phase delay of circadian entrainment. This cry-DASH may be a relevant piece of the complex regulatory mechanism governing circadian rhythmicity in *N. crassa*, and the subtle phenotypic change that its loss has under laboratory conditions could have an impact on the fitness of this fungus in nature. As found for *cryD*, the expression of the *cry* gene in *N. crassa* is strongly induced by light through the white collar complex. This complex plays a central role in the control of circadian rhythmicity (54), a phenomenon whose occurrence in *F. fujikuroi* has not been investigated.

A different biological role is noticeably played by the cry-DASH of *S. sclerotiorum*, Cry1. The expression of the *cry1* gene exhibits a tissue-specific regulation: its mRNA levels are low in vegetative mycelia and increase during development of apothecia,

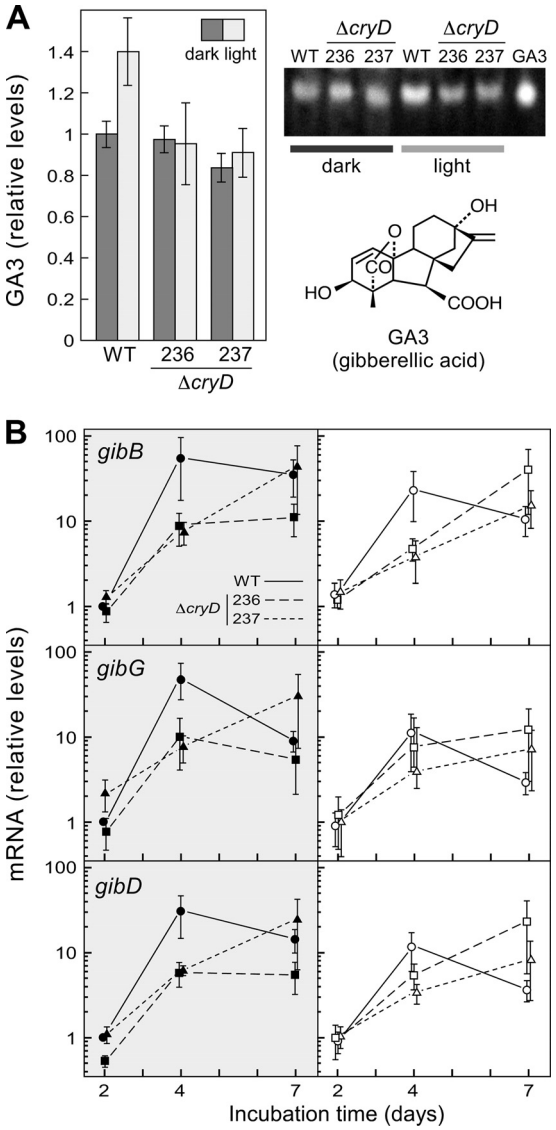

FIG 8 Effect of the Δ*cryD* mutation on GA production. (A) GA3 amounts in the filtrates of the wild type and the Δ*cryD* mutants SF236 and SF237grown for 7 days at 22°C or 30°C in low-N medium in the dark or under constant illumination. The right panel shows a representative example of the fluorescent spots on the TLC separation of gibberellin samples from the three strains, used for GA3 densitometry quantification. Lane GA3 contains gibberellic acid run as a control on the same TLC (chemical formula shown below). (B) qRT-PCR analyses for genes *gibB*, *gibD*, and *gibG* in RNA samples from the mycelia after 2, 4, and 7 days of incubation in low-N medium. Relative expression was referred to the value of the wild type in the dark. The data on GA3 production and *gib* mRNA levels show averages and standard errors from three independent experiments.

sexual reproduction structures formed during the life cycle of this fungus (52). In contrast to the cry-DASH genes of *F. fujikuroi* or *N. crassa*, exposure to visible light hardly affects the expression of *cry1* in *S. sclerotiorum*. However, it is strongly stimulated by exposure to UV-A wavebands, which also induce the maturation of apothecial stipes. The mutants carrying a *cry1* deletion exhibited minor developmental alterations, but still were able to produce normal apothecia, indicating that Cry1 plays a secondary role in the completion of the normal life cycle of *S. sclerotiorum* under laboratory conditions (52). In comparison, *N. crassa* protoperithecium formation and phototropism of perithecial beaks are induced by blue light through the WC system (55, 56), and none of these responses was apparently altered in the *cry* mutant (51).

The phenotypic alterations produced by the Δ*cryD* mutation in *F. fujikuroi* are different from those described for the counterpart mutants of *N. crassa* and *S. sclerotiorum*. The phenotypic changes of the *F. fujikuroi* mutants were only exhibited under blue light, in agreement with the *wcoA*-dependent expression of the *cryD* gene. Furthermore, the noticeable changes in pigmentation patterns, affecting more than one colored metabolite, indicate an unexpected participation of CryD in light regulation of secondary metabolism. This effect was quite manifest in the case of bikaverin production, derepressed under light in the Δ*cryD* mutants. The upregulation was particularly noticeable under nitrogen starvation, a major inducing signal for bikaverin biosynthesis in this fungus (8). This result involves CryD in the complex regulatory network governing nitrogen regulation of secondary metabolism in *F. fujikuroi*, and provides a link between nitrogen and light regulation. The regulatory role of CryD affects as well the synthesis of other metabolites, as suggested by the different pigmentation of the Δ*cryD* cultures in the light, due to unidentified pigments.

Our data also implicate CryD in the decision to make macroconidia. Little is known of the regulatory mechanisms governing this developmental process in *Fusarium*. Macroconidia are usually formed in large quantities by other *Fusarium* species (45), but they are rarely found in the cultures of our wild-type strain, which produces mostly microconidia as asexual spores. Our data suggest a role for CryD as a negative regulator of macroconidia production in *F. fujikuroi* and associate this regulatory function with nitrogen availability. However, the light-dependent repression roles of CryD in macroconidia and bikaverin production are not easy to interpret. Since functional CryD is only expected under illumination, the absence of macroconidia and the low bikaverin production in the dark suggest different repression systems operating in the dark and in the light for both processes.

Light induction on gibberellin production was formerly reported for two *F. fujikuroi* wild-type strains. In contrast to the 10- to 50-fold photoinduction of carotenoid biosynthesis, depending on strain and culture conditions (e.g., see references 6 and 44), the induction levels for gibberellin production were only 2-fold (57) and 1.4-fold (58). Our data showed about a 1.4-fold increase in GA3 production in the light compared to the dark, in good agreement with the reported stimulations and with our former data with the same wild-type strain (26). The induction was not apparent in the Δ*cryD* mutants, suggesting the mediation of the CryD photoreceptor in this photoresponse. The transcript analyses for three enzymatic genes of the pathway suggest that this regulation is not achieved on mRNA levels. Actually, mRNA contents for the three genes investigated reached higher levels in the dark than in the light, indicating the participation of CryD in other regulatory mechanism, possibly associated with mRNA translation or stability. A similar conclusion may be inferred from the lack of significant effect of the Δ*cryD* mutation on the mRNA levels of the structural *bik* genes. Taken together, our data point to CryD as a putative photoreceptor involved in posttranscriptional regulatory mechanisms of secondary metabolism in *F. fujikuroi*.

In addition to cry-DASHs, some cryptochrome or photolyase-like proteins were found to play regulatory functions in fungi. PHR1 from *Trichoderma atroviride* regulates its own transcrip-

tion, possibly modulating the activity of the white collar BLR1/BLR2 complex (59). Targeted mutation of *phl1* from *Cercospora zeae-maydis* alters the expression of other genes involved in DNA damage repair, including the putative photolyase gene *cpd1*, and causes abnormalities in development and secondary metabolism (60). Finally, deletion of *cryA* from *Aspergillus nidulans* causes the induction of regulatory genes of the sexual cycle and stimulated sexual fruiting body formation (61). CryA may be also involved in other light-regulated processes, as indicated by the induction of the *veA* gene in the *cryA* mutant (61). VeA is a component of the VelB/VeA/LaeA complex, which participates in the control of asexual development and secondary metabolism in *A. nidulans* (62). Interestingly, a similar velvet-like complex affects conidiation and secondary metabolism in *F. fujikuroi* (63), suggesting a possible regulatory connection with CryD.

The participation of cry-DASH proteins in circadian rhythmicity in *N. crassa*, apothecium development in *S. sclerotiorum*, and secondary metabolism and macroconidium formation in *F. fujikuroi* points to a considerable functional diversification of these predicted photoreceptors in ascomycete fungi. Not by chance, these fungi are model systems in the study of the aforementioned biological processes, and some degree of functional conservation might still exist. For example, a role of the *F. fujikuroi* or *S. sclerotiorum* cry-DASHs in circadian rhythmicity would be easily disregarded, since this process has not been investigated in these fungi. In the case of *F. fujikuroi*, the light-dependent effects of the *cryD* mutation may be explained by the light-dependent expression of the gene, but a direct photoreceptor activity has not been discarded. New experiments will be needed to investigate the photobiochemical properties of this protein. So far, our experiments, together with those of the formerly reported fungal cry-DASHs, demonstrate the functional versatility of these proteins in fungi, irrespective of their possible photoreceptor roles and should aim to extend these studies to new examples in other fungal species.

ACKNOWLEDGMENTS

We thank Alfred Batschauer and Richard Pokorny for valuable contributions to improve the text and Attila Ádám for plasmid pNTP2.

This research was supported by grants from the Spanish Government (Ministerio de Ciencia y Tecnología, projects BIO2006-01323 and BIO2009-11131) and the Andalusian Government (project P07-CVI-02813). Spanish grants included support from the European Union (European Regional Development Fund [ERDF]). M.C. and J.G.-M. are holders of graduate fellowships from the Spanish Ministerio de Educación, Cultura y Deporte and Ministerio de Ciencia y Tecnología, respectively.

REFERENCES

1. **Hoffmeister D, Keller NP.** 2007. Natural products of filamentous fungi: enzymes, genes, and their regulation. Nat. Prod. Rep. **24**:393–416.
2. **Desjardins AE, Proctor RH.** 2007. Molecular biology of *Fusarium* mycotoxins. Int. J. Food. Microbiol. **119**:47–50.
3. **Rademacher W.** 1997. Gibberellins, p 193–205. *In* Anke T (ed), Fungal biotechnology. Chapman & Hall, London, United Kingdom.
4. **Avalos J, Cerdá-Olmedo E, Reyes F, Barrero AF.** 2007. Gibberellins and other metabolites of *Fusarium fujikuroi* and related fungi. Curr. Org. Chem. **11**:721–737.
5. **Limón MC, Rodríguez-Ortiz R, Avalos J.** 2010. Bikaverin production and applications. Appl. Microbiol. Biotechnol. **87**:21–29.
6. **Avalos J, Cerdá-Olmedo E.** 1987. Carotenoid mutants of *Gibberella fujikuroi*. Curr. Genet. **25**:1837–1841.
7. **Tudzynski B.** 2005. Gibberellin biosynthesis in fungi: genes, enzymes, evolution, and impact on biotechnology. Appl. Microbiol. Biotechnol. **66**:597–611.
8. **Wiemann P, Willmann A, Straeten M, Kleigrewe K, Beyer M, Humpf HU, Tudzynski B.** 2009. Biosynthesis of the red pigment bikaverin in *Fusarium fujikuroi*: genes, their function and regulation. Mol. Microbiol. **72**:931–946.
9. **Avalos J, Estrada AF.** 2010. Regulation by light in *Fusarium*. Fungal Genet. Biol. **47**:930–938.
10. **Rodríguez-Ortiz R, Limón MC, Avalos J.** 2009. Regulation of carotenogenesis and secondary metabolism by nitrogen in wild-type *Fusarium fujikuroi* and carotenoid-overproducing mutants. Appl. Environ. Microbiol. **75**:405–413.
11. **Mihlan M, Homann V, Liu T-WD, Tudzynski B.** 2003. AREA directly mediates nitrogen regulation of gibberellin biosynthesis in *Gibberella fujikuroi*, but its activity is not affected by NMR. Mol. Microbiol. **47**:975–991.
12. **Schönig B, Brown DW, Oeser B, Tudzynski B.** 2008. Cross-species hybridization with *Fusarium verticillioides* microarrays reveals new insights into *Fusarium fujikuroi* nitrogen regulation and the role of AreA and NMR. Eukaryot. Cell **7**:1831–1846.
13. **Muñoz GA, Agosin E.** 1993. Glutamine involvement in nitrogen control of gibberellic acid production in *Gibberella fujikuroi*. Appl. Environ. Microbiol. **59**:4317–4322.
14. **Teichert S, Schonig B, Richter S, Tudzynski B.** 2004. Deletion of the *Gibberella fujikuroi* glutamine synthetase gene has significant impact on transcriptional control of primary and secondary metabolism. Mol. Microbiol. **53**:1661–1675.
15. **Teichert S, Rutherford JC, Wottawa M, Heitman J, Tudzynski B.** 2008. Impact of ammonium permeases MepA, MepB, and MepC on nitrogen-regulated secondary metabolism in *Fusarium fujikuroi*. Eukaryot. Cell **7**:187–201.
16. **Giordano W, Avalos J, Cerdá-Olmedo E, Domenech CE.** 1999. Nitrogen availability and production of bikaverin and gibberellins in *Gibberella fujikuroi*. FEMS Microbiol. Lett. **173**:389–393.
17. **Wagner D, Schmeinck A, Mos M, Morozov IY, Caddick MX, Tudzynski B.** 2010. The bZIP transcription factor MeaB mediates nitrogen metabolite repression at specific loci. Eukaryot. Cell **9**:1588–1601.
18. **Corrochano LM, Avalos J.** 2010. Light sensing, p 417–441. *In* Borkovich K, Ebbole D, Momany M (ed), Cellular and molecular biology of filamentous fungi. ASM Press, Washington, DC.
19. **Idnurm A, Verma S, Corrochano LM.** 2010. A glimpse into the basis of vision in the kingdom Mycota. Fungal Genet. Biol. **47**:881–892.
20. **Navarro-Sampedro L, Yanofsky C, Corrochano LM.** 2008. A genetic selection for *Neurospora crassa* mutants altered in their light regulation of transcription. Genetics **178**:171–183.
21. **Salgado LM, Avalos J, Bejarano ER, Cerdá-Olmedo E.** 1991. Correlation between in vivo and in vitro carotenogenesis in *Phycomyces*. Phytochemistry **30**:2587–2591.
22. **Chen CH, Dunlap JC, Loros JJ.** 2010. *Neurospora* illuminates fungal photoreception. Fungal Genet. Biol. **47**:922–929.
23. **Ballario P, Macino G.** 1997. White collar proteins: PASsing the light signal in *Neurospora crassa*. Trends Microbiol. **5**:458–462.
24. **He Q, Cheng P, Yang Y, Wang L, Gardner KH, Liu Y.** 2002. White collar-1, a DNA binding transcription factor and a light sensor. Science **297**:840–843.
25. **Corrochano LM.** 2007. Fungal photoreceptors: sensory molecules for fungal development and behaviour. Photochem. Photobiol. Sci. **6**:725–736.
26. **Estrada AF, Avalos J.** 2008. The White Collar protein WcoA of *Fusarium fujikuroi* is not essential for photocarotenogenesis, but is involved in the regulation of secondary metabolism and conidiation. Fungal Genet. Biol. **45**:705–718.
27. **Ruiz-Roldán MC, Garre V, Guarro J, Mariné M, Roncero MI.** 2008. Role of the white collar 1 photoreceptor in carotenogenesis, UV resistance, hydrophobicity, and virulence of *Fusarium oxysporum*. Eukaryot. Cell **7**:1227–1230.
28. **Chaves I, Pokorny R, Byrdin M, Hoang N, Ritz T, Brettel K, Essen LO, van der Horst GT, Batschauer A, Ahmad M.** 2011. The cryptochromes: blue light photoreceptors in plants and animals. Annu. Rev. Plant Biol. **62**:335–364.
29. **Sancar A.** 2003. Structure and function of DNA photolyase and cryptochrome blue-light photoreceptors. Chem. Rev. **103**:2203–2237.
30. **Díaz-Sánchez V, Estrada AF, Trautmann D, Al-Babili S, Avalos J.** 2011.

The gene *carD* encodes the aldehyde dehydrogenase responsible for neurosporaxanthin biosynthesis in *Fusarium fujikuroi*. FEBS J. **278**:3164–3176.
31. **Avalos J, Casadesús J, Cerdá-Olmedo E.** 1985. *Gibberella fujikuroi* mutants obtained with UV radiation and *N*-methyl-*N*′-nitro-*N*-nitrosoguanidine. Appl. Environ. Microbiol. **49**:187–191.
32. **Geissman TA, Verbiscar AJ, Phinney BO, Cragg G.** 1966. Studies on the biosynthesis of gibberellins from (−)-kaurenoic acid in cultures of *Gibberella fujikuroi*. Phytochemistry **5**:933–947.
33. **Punt PJ, Oliver RP, Dingemanse MA, Pouwels PH, van den Hondel CA.** 1987. Transformation of *Aspergillus* based on the hygromycin B resistance marker from *Escherichia coli*. Gene **56**:117–124.
34. **Proctor RH, Hohn TM, McCormick SP.** 1997. Restoration of wild-type virulence to Tri5 disruption mutants of *Gibberella zeae* via gene reversion and mutant complementation. Microbiology **143**:2583–2591.
35. **Weinkove D, Poyatos JA, Greiner H, Oltra E, Avalos J, Fukshansky L, Barrero AF, Cerdá-Olmedo E.** 1998. Mutants of *Phycomyces* with decreased gallic acid content. Fungal Genet. Biol. **25**:196–203.
36. **Sambrook J, Russell DW.** 2001. Molecular cloning: a laboratory manual, 3rd ed. Cold Spring Harbor Laboratory Press, New York, NY.
37. **Arrach N, Schmidhauser TJ, Avalos J.** 2002. Mutants of the carotene cyclase domain of *al-2* from *Neurospora crassa*. Mol. Genet. Genomics **266**:914–921.
38. **Balan J, Fuska J, Kuhr I, Kuhrová V.** 1970. Bikaverin, an antibiotic from *Gibberella fujikuroi*, effective against *Leishmania brasiliensis*. Folia Microbiol. (Praha) **15**:479–484.
39. **Bhalla K, Singh SB, Agarwal R.** 2010. Quantitative determination of gibberellins by high performance liquid chromatography from various gibberellins producing *Fusarium* strains. Environ. Monit. Assess. **167**:515–520.
40. **García-Martínez J, Ádám AL, Avalos J.** 2012. Adenylyl cyclase plays a regulatory role in development, stress resistance and secondary metabolism in *Fusarium fujikuroi*. PLoS One **7**:e28849. doi:10.1371/journal.pone.0028849.
41. **Prado MM, Prado-Cabrero A, Fernández-Martín R, Avalos J.** 2004. A gene of the opsin family in the carotenoid gene cluster of *Fusarium fujikuroi*. Curr. Genet. **46**:47–58.
42. **Thompson JD, Gibson TJ, Plewniak F, Jeanmougin F, Higgins DG.** 1997. The ClustalX Windows interface: flexible strategies for multiple sequence alignment aided by quality analysis tools. Nucleic Acids Res. **24**:4876–4882.
43. **Schultz J, Milpetz F, Bork P, Ponting CP.** 1998. SMART, a simple modular architecture research tool: identification of signaling domains. Proc. Natl. Acad. Sci. U. S. A. **95**:5857–5864.
44. **Estrada AF, Avalos J.** 2009. Regulation and targeted mutation of *opsA*, coding for the NOP-1 opsin orthologue in *Fusarium fujikuroi*. J. Mol. Biol. **387**:59–73.
45. **Leslie JF, Summerell BA.** 2006. The *Fusarium* laboratory manual. Blackwell Professional, Ames, IA.
46. **Linnemannstöns P, Schulte J, Prado MM, Proctor RH, Avalos J, Tudzynski B.** 2002. The polyketide synthase gene *pks4* from *Gibberella fujikuroi* encodes a key enzyme in the biosynthesis of the red pigment bikaverin. Fungal Genet. Biol. **37**:134–148.
47. **Candau R, Avalos J, Cerdá-Olmedo E.** 1992. Regulation of gibberellin biosynthesis in *Gibberella fujikuroi*. Plant Physiol. **100**:1184–1188.
48. **Sancar A.** 2004. Photolyase and cryptochrome blue-light photoreceptors. Adv. Protein Chem. **69**:73–100.
49. **Oberpichler I, Pierik AJ, Wesslowski J, Pokorny R, Rosen R, Vugman M, Zhang F, Neubauer O, Ron EZ, Batschauer A, Lamparter T.** 2011. A photolyase-like protein from *Agrobacterium tumefaciens* with an iron-sulfur cluster. PLoS One **6**:e26775. doi:10.1371/journal.pone.0026775.
50. **Brudler R, Hitomi K, Daiyasu H, Toh H, Kucho K, Ishiura M, Kanehisa M, Roberts VA, Todo T, Tainer JA, Getzoff ED.** 2003. Identification of a new cryptochrome class. Structure, function, and evolution. Mol. Cell **11**:59–67.
51. **Froehlich AC, Chen CH, Belden WJ, Madeti C, Roenneberg T, Merrow M, Loros JJ, Dunlap JC.** 2010. Genetic and molecular characterization of a cryptochrome from the filamentous fungus *Neurospora crassa*. Eukaryot. Cell **9**:738–750.
52. **Veluchamy S, Rollins JA.** 2008. A CRY-DASH-type photolyase/cryptochrome from *Sclerotinia sclerotiorum* mediates minor UV-A-specific effects on development. Fungal Genet. Biol. **45**:1265–1276.
53. **Chen CH, Loros JJ.** 2009. *Neurospora* sees the light: light signaling components in a model system. Commun. Integr. Biol. **2**:448–451.
54. **Dunlap JC, Loros JJ.** 2004. The *Neurospora* circadian system. J. Biol. Rhythms **19**:414–424.
55. **Degli-Innocenti F, Russo VE.** 1984. Isolation of new white collar mutants of *Neurospora crassa* and studies on their behavior in the blue light-induced formation of protoperithecia. J. Bacteriol. **159**:757–761.
56. **Harding RW, Melles S.** 1983. Genetic analysis of phototropism of *Neurospora crassa* perithecial beaks using white collar and albino mutants. Plant Physiol. **72**:996–1000.
57. **Mertz D, Henson W.** 1967. Light stimulated biosynthesis of gibberellins in *Fusarium moniliforme*. Nature **214**:844–846.
58. **Johnson SW, Coolbaugh RC.** 1990. Light-stimulated gibberellin biosynthesis in *Gibberella fujikuroi*. Plant Physiol. **94**:1696–1701.
59. **Berrocal-Tito GM, Esquivel-Naranjo EU, Horwitz BA, Herrera-Estrella A.** 2007. *Trichoderma atroviride* PHR1, a fungal photolyase responsible for DNA repair, autoregulates its own photoinduction. Eukaryot. Cell **6**:1682–1692.
60. **Bluhm BH, Dunkle LD.** 2008. PHL1 of *Cercospora zeae-maydis* encodes a member of the photolyase/cryptochrome family involved in UV protection and fungal development. Fungal Genet. Biol. **45**:1364–1372.
61. **Bayram Ö, Biesemann C, Krappmann S, Galland P, Braus GH.** 2008. More than a repair enzyme: *Aspergillus nidulans* photolyase-like CryA is a regulator of sexual development. Mol. Biol. Cell **19**:3254–3262.
62. **Bayram Ö, Krappmann S, Ni M, Bok JW, Helmstaedt K, Valerius O, Braus-Stromeyer S, Kwon NJ, Keller NP, Yu JH, Braus GH.** 2008. VelB/VeA/LaeA complex coordinates light signal with fungal development and secondary metabolism. Science **320**:1504–1506.
63. **Wiemann P, Brown DW, Kleigrewe K, Bok JW, Keller NP, Humpf HU, Tudzynski B.** 2010. FfVel1 and FfLae1, components of a *velvet*-like complex in *Fusarium fujikuroi*, affect differentiation, secondary metabolism and virulence. Mol. Microbiol. **77**:972–994.